

## Quasiblack holes from extremal charged dust

José P. S. Lemos\*

*Physics Department, Columbia University, New York, New York 10027, USA  
and Centro Multidisciplinar de Astrofísica, CENTRA, Departamento de Física, Instituto Superior Técnico, Universidade Técnica de Lisboa, Av. Rovisco Pais 1, 1049-001 Lisboa, Portugal*

Erick J. Weinberg†

*Physics Department, Columbia University, New York, New York 10027, USA*

(Received 15 November 2003; published 12 May 2004)

One can construct families of static solutions that can be viewed as interpolating between nonsingular spacetimes and those containing black holes. Although everywhere nonsingular, these solutions come arbitrarily close to having a horizon. To an observer in the exterior region, it becomes increasingly difficult to distinguish these from a true black hole as the critical limiting solution is approached. In this paper we use the Majumdar-Papapetrou formalism to construct such quasi-black hole solutions from extremal charged dust. We study the gravitational properties of these solutions, comparing them with the quasi-black hole solutions based on magnetic monopoles. As in the latter case, we find that solutions can be constructed with or without hair.

DOI: 10.1103/PhysRevD.69.104004

PACS number(s): 04.20.Jb, 04.70.Bw

### I. INTRODUCTION

Nonsingular spacetimes and those containing black holes are usually viewed as being qualitatively quite distinct. However, one can construct families of static solutions that can be viewed as interpolating between these two types of spacetimes. Although these solutions remain nonsingular, they come arbitrarily close to having a horizon. To an observer in the “exterior” region, it becomes increasingly difficult to distinguish these from a true black hole as the critical limiting solution is approached. These solutions provide a useful theoretical laboratory for studying the properties of true black holes [1], and can lead to insight into the nature of black hole entropy [2].

To make this more concrete, consider a spherically symmetric spacetime with a metric of the form

$$ds^2 = -B(r)dt^2 + A(r)dr^2 + r^2(d\theta^2 + \sin^2\theta d\phi^2). \quad (1.1)$$

If the spacetime is asymptotically flat, as we will assume in this paper, we can set  $B(\infty) = A(\infty) = 1$ . A horizon corresponds to a zero of  $A^{-1}$ . If  $dA^{-1}/dr$  also vanishes, the horizon is extremal. By a quasi-black hole solution, we will mean one that is everywhere nonsingular and for which  $A^{-1}$  has a minimum value  $A^{-1}(r_*) = \epsilon$  that can be adjusted to be arbitrarily close to zero. We will refer to the location of this minimum,  $r_*$ , as the quasihorizon. An external observer orbiting at some fixed radius  $r_0 \gg r_*$  could try to explore the “interior” region  $r < r_*$  by sending in a series of probes and waiting for them to emerge. Because the spacetime is nonsingular, these probes would eventually return to the observer. However, the minimum time delay (as measured in terms of the external observer’s proper time) between the

launch and the return of such probes diverges as  $\epsilon$  tends toward zero. Thus, given a fixed finite observing time, the external observer would not be able to distinguish between nonsingular solutions sufficiently close to the critical limit  $\epsilon = 0$  and true black holes.

To see how such a solution might come about, consider a static spacetime with a spherically symmetric concentration of matter near the origin,  $r = 0$ . If the spacetime is nonsingular, then  $A(0) = 1$ . As one moves out from the origin,  $A^{-1}$  initially decreases until it reaches a minimum value, typically at a radius near the edge of the mass distribution, and then increases toward its asymptotic value. The minimum of  $A^{-1}$  becomes deeper as the density of the mass distribution is increased. This suggests that one could approach the black hole limit simply by making the density large enough. The difficulty, of course, is in finding a form of matter that can withstand the increasing gravitational forces and avoid gravitational collapse. For example, this program cannot succeed with a star composed of a fluid described by an equation of state  $p = p(\rho)$  with the density  $\rho$  and pressure  $p$  obeying standard conditions.

The quasi-black holes studied in Ref. [1] were constructed by invoking the classical magnetic monopole solutions that arise in spontaneously broken gauge theories. If the parameters of the theory are varied in such a way as to increase the Higgs expectation value  $v$ , the monopole mass increases, while its core radius decreases. These two effects combine to lower the minimum of  $A^{-1}$ . At a value  $v_{\text{cr}}$  of the order of the Planck mass, the critical limit is reached and the nonsingular monopole goes over into a black hole with horizon radius  $r_{\text{H}} \sim 1/ev$  [3–8].

In this paper we will study quasi-black hole solutions obtained from a much less exotic form of matter. We will use charged dust; i.e., pressureless matter carrying nonzero electric charge, with its behavior described by the coupled Einstein-Maxwell equations. More specifically, we take the special case of extremal dust, where the energy density (in Planck units) is everywhere equal to the charge density.

\*Electronic address: lemos@kelvin.ist.utl.pt

†Electronic address: ejw@phys.columbia.edu

Within the context of Newtonian gravity, any static distribution of this dust would clearly be stable, since the gravitational attraction between particles would exactly cancel their Coulomb repulsion. The situation is perhaps less obvious in general relativity, both because the simple Newtonian force law description is lost and because the gravitational effects of the energy density in the electric field must be taken into account. Nevertheless, it was shown by Majumdar [9] and Papapetrou [10] that the Newtonian result does in fact generalize.

Solutions of the Majumdar-Papapetrou system with extremal charged dust were investigated further by Bonnor and Wickramasuriya [11,12], who pointed out that these solutions can come arbitrarily close to being black holes. In this article we will examine this possibility in some detail, paying particular attention to the interior region of the solution, and comparing the gravitational properties of these quasi-black holes with those based on magnetic monopoles. We will also investigate whether, as in the case of the quasi-black holes built from monopoles, there are two classes of solutions, with one possessing hair and being less singular than the other [1,8].

The remainder of the paper is organized as follows. In Sec. II we describe the general formalism that we use and present some basic formulas. In Sec. III, we present a family of quasi-black hole solutions whose exterior region tends toward that of an extremal Reissner-Nordström black hole. In Sec. IV we discuss the possibility of solutions with hair. We sum up briefly in Sec. V.

## II. BASIC EQUATIONS

### A. Equations in harmonic coordinates

For charged dust the gravitational field equation takes the form

$$G_{ab} = 8\pi(T_{ab}^{\text{dust}} + T_{ab}^{\text{em}}), \quad (2.1)$$

where  $G_{ab}$  is the Einstein tensor and we have set  $G = c = 1$ . The dust part of the stress-energy tensor is

$$T_{ab}^{\text{dust}} = \rho u_a u_b, \quad (2.2)$$

with  $\rho$  being the energy density and  $u_a$  the four-velocity of the fluid. The electromagnetic part of the stress-energy tensor is

$$T_{ab}^{\text{em}} = \frac{1}{4\pi} \left( F_a^c F_{bc} - \frac{1}{4} g_{ab} F^{cd} F_{cd} \right), \quad (2.3)$$

where the electromagnetic field strength

$$F_{ab} = A_{a,b} - A_{b,a} \quad (2.4)$$

satisfies

$$F^{ab}{}_{;b} = 4\pi j^a = 4\pi \rho_e u^a, \quad (2.5)$$

with  $\rho_e$  the electric charge density of the dust.

For a static purely electric system one can make the choice

$$u^a = \delta_0^a U, \quad A_a = \delta_a^0 \varphi. \quad (2.6)$$

Here  $\varphi$  and  $U$  are functions of the spatial coordinates, with  $\varphi$  being the electric potential and  $U^{-1} - 1$  being the gravitational potential in the Newtonian limit. Furthermore, in a very elegant paper [9] Majumdar showed that in the special case of extremal dust,

$$\rho_e = \rho, \quad (2.7)$$

the metric can be put in the form

$$ds^2 = -\frac{dt^2}{U^2} + U^2(dx^2 + dy^2 + dz^2), \quad (2.8)$$

where  $(t, x, y, z)$  are called harmonic coordinates. The Einstein-Maxwell equations (2.1) and (2.5) then reduce to the pair of equations

$$\left( \frac{\partial^2}{\partial x^2} + \frac{\partial^2}{\partial y^2} + \frac{\partial^2}{\partial z^2} \right) U = -4\pi \rho U^3 \quad (2.9)$$

and

$$\varphi = -\frac{1}{U} + 1. \quad (2.10)$$

Note that the second of these reduces in the Newtonian limit to the requirement that the gravitational and electric potentials be equal.<sup>1</sup>

Solutions of this Maxwell-Einstein-extremal-dust system are generically called Majumdar-Papapetrou solutions [9,10]. In particular, the vacuum solutions, with  $\rho = \rho_e = 0$ , reduce to a configuration of many extreme Reissner-Nordström black holes, as was fully explored by Hartle and Hawking [13]. Solutions with matter have been examined in the papers of Das [14], Bonnor [11,12], and others (see Ref. [15] and the references cited therein).

Although solutions of Eq. (2.9) need not have any spatial symmetry at all, we will focus on spherically symmetric solutions, for which the line element (2.8) can be rewritten as

$$ds^2 = -\frac{dt^2}{U^2} + U^2[dR^2 + R^2(d\theta^2 + \sin^2\theta d\phi^2)], \quad (2.11)$$

where  $U = U(R)$ . Equation (2.9) then takes the form

$$\frac{1}{R^2} \frac{\partial}{\partial R} \left( R^2 \frac{\partial U}{\partial R} \right) = -4\pi U^3 \rho. \quad (2.12)$$

This equation can be solved by guessing a potential  $U$ , and then finding  $\rho$ . The solution is then complete because  $\rho_e$  and

<sup>1</sup>An arbitrary choice of sign was made in Eq. (2.7). If we had chosen to consider extremal dust with  $\rho_e = -\rho$ , the only change would be to replace  $\varphi$  by  $-\varphi$  in Eq. (2.10).

$\varphi$  follow directly. In order that the solution be physically acceptable, it must satisfy the additional requirement that  $\rho$  be everywhere nonnegative.

### B. Equations in Schwarzschild coordinates

Although the field equations are most easily solved by working in harmonic coordinates, the physical interpretation of the solutions is clearer if one uses the Schwarzschild coordinates defined by the line element of Eq. (1.1). By comparing Eqs. (1.1) and (2.11), we see that the radial coordinates in the two systems are related by

$$r = UR \quad (2.13)$$

and that the metric components are related by

$$B = \frac{1}{U^2} \quad (2.14)$$

and

$$\frac{1}{\sqrt{A}} = 1 + \frac{R}{U} \frac{dU}{dR}. \quad (2.15)$$

Note that Eq. (2.13) gives  $r$  as a function of  $R$ . Although this implicitly determines  $R$  as a function of  $r$ , it is only in special cases that this can be done explicitly.

For later reference, we present here the Schwarzschild coordinate form of the field equations. With the metric in the form of Eq. (1.1), Eqs. (2.1)–(2.5) reduce to

$$\frac{(AB)'}{AB} = 8\pi r \rho A, \quad (2.16)$$

$$\left[ r \left( 1 - \frac{1}{A} \right) \right]' = 8\pi r^2 \rho + \frac{r^2}{AB} \varphi'^2, \quad (2.17)$$

$$\frac{\sqrt{B}}{r^2 \sqrt{AB}} \left[ \frac{r^2}{\sqrt{AB}} \varphi' \right]' = -4\pi \rho_e, \quad (2.18)$$

where primes denote differentiation with respect to  $r$ .

### C. Examples

Finally, we present two simple solutions. The first corresponds to vanishing density. With  $\rho = 0$ , the general solution of Eq. (2.12) takes the form  $U = k + q/R$ , where  $k$  and  $q$  are constants of integration. Without any loss of generality, we can rescale coordinates and adjust the overall sign of  $U$  to set  $k = 1$  and make  $q$  positive, obtaining

$$U_{\text{RN}} = 1 + \frac{q}{R}. \quad (2.19)$$

Equations (2.13)–(2.15) then give

$$r = R + q \quad (2.20)$$

and

$$B = \frac{1}{A} = \left( \frac{R}{R+q} \right)^2 = \left( 1 - \frac{q}{r} \right)^2. \quad (2.21)$$

We recognize this as the metric for an extremal Reissner-Nordström black hole with charge and mass equal to  $q$ .

Some comment on the range of the radial coordinates is in order here. For a nonsingular solution with no horizon, the natural range of  $r$  is  $0 \leq r < \infty$ . Since  $B = 1/U^2$  is everywhere nonzero and finite, Eq. (2.13) maps the range  $0 \leq r < \infty$  to  $0 \leq R < \infty$ . When there is a horizon, the vanishing of  $B$  at the horizon produces a divergence in  $U$  that can allow  $r$  to remain nonzero at  $R = 0$ . This is precisely what happens for the Reissner-Nordström solution, where  $R > 0$  covers only the region outside the horizon; the region inside the horizon is obtained by continuing the solution to the range  $-q \leq R < 0$ .

A less trivial solution [11,12] is the Bonnor star, for which

$$U = \begin{cases} 1 + \frac{m}{R_b} \left( \frac{3}{2} - \frac{R^2}{2R_b^2} \right), & R < R_b, \\ 1 + \frac{m}{R}, & R > R_b. \end{cases} \quad (2.22)$$

This corresponds to a density

$$\rho = \begin{cases} \frac{3m}{4\pi R_b^3 U^3}, & R < R_b, \\ 0, & R > R_b. \end{cases} \quad (2.23)$$

Note that in the region outside the mass distribution the Bonnor solution takes the Reissner-Nordström form. This result carries over to a more general situation. Whenever the matter density  $\rho$  vanishes identically for all  $R$  greater than some value  $R_b$ , then for all  $R > R_b$  we have  $U(R) = 1 + m/R$ . Integration of Eq. (2.12) shows that the constant  $m$  is given by

$$m = 4\pi \int_0^{R_b} dR R^2 U^3 \rho + m_0 = 4\pi \int_{r_0}^{r_b} dr r^2 \sqrt{A} \rho + m_0 \quad (2.24)$$

where  $r_0 = r(R = 0)$  and  $m_0$  is an integration constant. For a nonsingular spacetime  $m_0 = 0$  and  $m$  is equal to the spatial integral (with the correct volume element) of the matter density. (Recall that the factor of  $\sqrt{A}$  is absent from the analogous formula for neutral dust. This can be viewed as being due to the contribution of gravitational potential energy to the total mass. For extremal dust the energy in the electric field precisely cancels the gravitational potential energy and restores the factor of  $\sqrt{A}$ .) For the Reissner-Nordström black hole, on the other hand, the matter density vanishes identically and  $m$  comes entirely from  $m_0$ , which can be viewed as the contribution from the singularity at  $r = 0$ .

**III. QUASI-REISSNER-NORDSTRÖM SOLUTIONS**

We now want to find nonsingular solutions that can be viewed as quasi-black holes. We start, in this section, by seeking a family of solutions that will, in some sense, tend toward the extremal Reissner-Nordström solution.

One possible approach would be to first postulate a density profile and then solve Eq. (2.12) to obtain the metric. Even aside from the possible difficulties in solving this differential equation, the identically vanishing  $\rho$  of the Reissner-Nordström solution does not give us any useful hints as to what density profile we should choose.

We therefore try a different approach. Working in harmonic coordinates, we start by postulating a family of profiles for  $U(R)$  that includes the Reissner-Nordström case, Eq. (2.19), as a limiting case. Specifically, we take<sup>2</sup>

$$U = 1 + \frac{q}{\sqrt{R^2 + c^2}}. \tag{3.1}$$

When  $c=0$ , this reduces to Eq. (2.19), with the horizon lying at  $R=0$  and  $r=q$ . For any finite  $c$ , on the other hand, it gives a nonsingular spacetime, with the origin at  $R=r=0$ . For  $R/c$  sufficiently large, we might expect this spacetime to approximate the Reissner-Nordström solution.

As described in the previous section, any choice for  $U(R)$  gives a solution of the Einstein equations. However, to make sure that the solution is physically acceptable, we must check that the density  $\rho$  is everywhere positive.<sup>3</sup> Substituting Eq. (3.1) into Eq. (2.12), we obtain

$$\rho = \frac{1}{4\pi} \frac{3qc^2}{(R^2 + c^2)[q + \sqrt{R^2 + c^2}]^3}. \tag{3.2}$$

This is indeed positive definite, as required. At short distances ( $R \ll c$ ), the density is approximately constant, but when  $R$  is greater than both  $q$  and  $c$  the density falls rapidly, as  $1/R^5$ .

To explore the existence of a horizon or a quasihorizon, we need the Schwarzschild metric component  $g^{rr} = 1/A$ . Using Eq. (2.15), we find that

$$\frac{1}{\sqrt{A}} = 1 - \frac{qR^2}{(R^2 + c^2)[q + \sqrt{R^2 + c^2}]}, \tag{3.3}$$

where  $R$  should be viewed as a function of  $r$ . For  $R \gg c$ , this differs from the Reissner-Nordström result by terms that are no greater than  $c^2/R^2$ . For small  $R$ , on the other hand, the behavior is quite different. Rather than finding a pole at  $R=0$ , we see that  $1/\sqrt{A}$  differs from unity by terms of order

<sup>2</sup>For another possible choice, see Ref. [12].  
<sup>3</sup>As evidence that this is a nontrivial requirement, we note that the choice  $U = 1 + q(R^2 + c^2)^{-\gamma}$  gives a negative energy density if  $\gamma > 1/2$ . If  $\gamma < 1/2$ , the density is positive, and  $1/A$  is bounded from below by  $1 - 2\gamma$ .

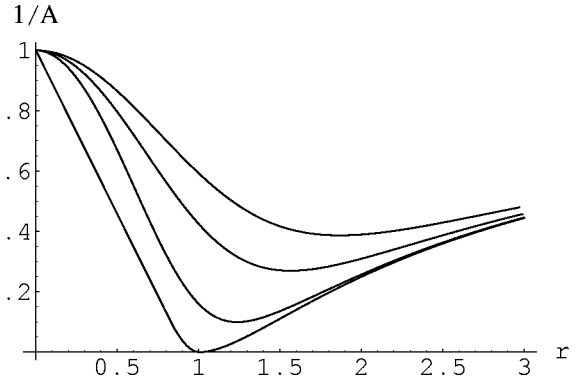


FIG. 1. A plot of  $1/A$  as a function of  $r$  for  $q=1$  and, reading from the top down,  $c=0.5, 0.3, 0.1, 0.001$ . The emergence of the quasihorizon is quite evident in the  $c=0.001$  curve.

$R^2$ , just as would be expected for a nonsingular configuration with finite density near the origin.

Differentiation of Eq. (3.3) shows that  $1/\sqrt{A}$  has a minimum at  $R=R_*$ , where  $R_*$  satisfies

$$\frac{2q}{c} = \left( \frac{R_*^2}{c^2} - 2 \right) \sqrt{\frac{R_*^2}{c^2} + 1}. \tag{3.4}$$

For  $c \ll q$  this gives

$$R_* = \left( \frac{2c^2}{q^2} \right)^{1/3} q \left[ 1 + O\left( \frac{c^{2/3}}{q^{2/3}} \right) \right] \ll q. \tag{3.5}$$

Substituting these results back into Eq. (3.3), we find that the minimum of  $1/A$  is

$$\epsilon = \frac{1}{A(R_*)} = \left( \frac{3c^2}{R_*^2 + c^2} \right)^2 = 9 \left( \frac{c}{2q} \right)^{4/3} + \dots \tag{3.6}$$

This vanishes as  $c \rightarrow 0$ , and so Eq. (3.1) does indeed generate quasi-black hole solutions. Furthermore, in the region outside the quasihorizon  $1/A$  approaches the extremal Reissner-Nordström result as  $c \rightarrow 0$ .

Although the use of harmonic coordinates simplified the task of finding these solutions, these coordinates are not well

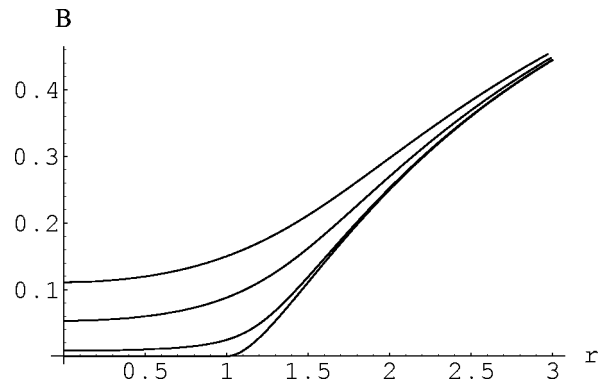


FIG. 2. A plot of  $B(r)$  for  $q=1$  and, reading from the top down,  $c=0.5, 0.3, 0.1, 0.001$ .

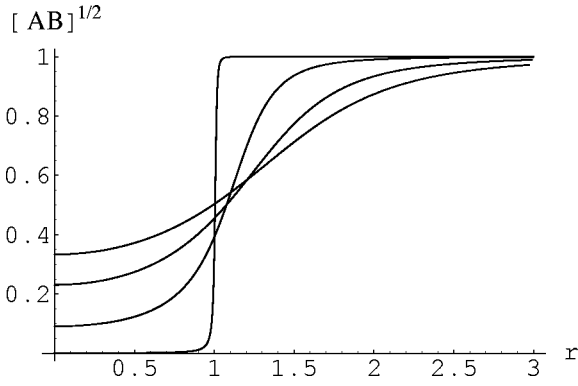


FIG. 3. A plot of  $\sqrt{AB}$  as a function of  $r$  for  $q=1$  and, reading from the top down along the vertical axis,  $c=0.5, 0.3, 0.1, 0.001$ . Note that for  $c=0.001$ ,  $\sqrt{AB}$  is virtually zero in the whole interior of the quasi-black hole solution.

suit for studying their properties near the critical limit. To see this, note that Eq. (3.5) implies that  $R_* \rightarrow 0$  as  $c \rightarrow 0$ . Hence, when viewed in harmonic coordinates, the region  $0 < R < R_*$  inside the quasihorizon seems to collapse to a point in the critical limit. This difficulty can be avoided by using the Schwarzschild coordinate

$$r = RU = R + \frac{qR}{\sqrt{R^2 + c^2}} \quad (3.7)$$

because the behavior of  $U$  near the critical limit has the effect of stretching the interior region back to its “natural” size. From Eqs. (3.5) and (3.7) we find that

$$r_* = q \left[ 1 + \frac{3}{4} \left( \frac{2c^2}{q^2} \right)^{1/3} + \dots \right] \quad (3.8)$$

so that the Schwarzschild radial coordinate of the quasihorizon is approximately constant as the critical limit is approached.

More generally, inversion of Eq. (3.7) gives the limiting cases

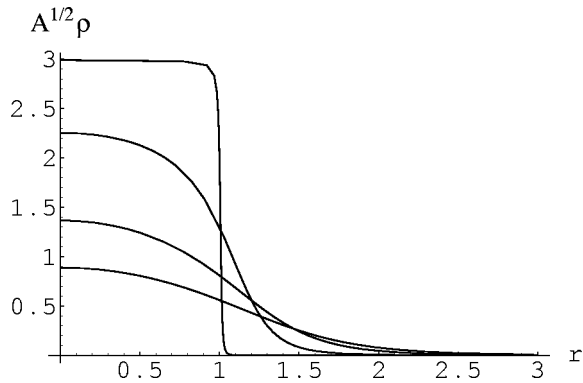


FIG. 4. A plot of  $\sqrt{A}\rho$  as a function of  $r$  for  $q=1$  and, reading from the bottom up along the vertical axis,  $c=0.5, 0.3, 0.1, 0.001$ . Note that for  $c=0.001$  the density is essentially constant up to the quasihorizon radius and then drops sharply toward zero, showing that this is a no-hair solution.

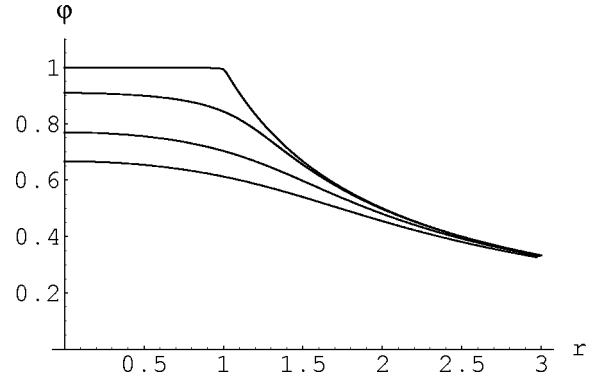


FIG. 5. A plot of  $\phi(r)$  for  $q=1$  and, reading from the bottom up,  $c=0.5, 0.3, 0.1, 0.001$ . Note that for  $c=0.001$  the potential is essentially constant up to the horizon and then drops as  $1/r$ , as required for a no-hair solution.

$$R = \begin{cases} \frac{cr}{q+c} + O(r^3/q^2), & R \ll c, \\ r - q + O(qc^2/r^3), & R \gg R_* . \end{cases} \quad (3.9)$$

In Fig. 1 we plot  $1/A$  as a function of  $r$  for several values of  $c$ . Its behavior is just as expected, starting from unity at the origin, decreasing to a minimum value, and then increasing at large distance toward an asymptotic value of unity. It remains everywhere smooth in the critical limit, differing from the extremal Reissner-Nordström solution in not having a singularity at  $r=0$ . The behavior of  $B$  is shown in Fig. 2. For a black hole,  $B$  should vanish at the horizon. Indeed,  $B(r_*) \approx (2c^2/q^2)^{2/3}$  tends to zero in the critical limit. However,  $B$  does not have a minimum at the quasihorizon, but rather decreases monotonically as  $r \rightarrow 0$ . In the limiting case,  $B$  is identically zero for all  $r < r_*$ . Similarly,  $\sqrt{AB}$ , shown in Fig. 3, also vanishes identically in the interior region in the critical limit. Hence, although we have a nonsingular spacetime for all nonzero  $c$ , the limiting case  $c=0$  is not itself a smooth manifold.

It is also interesting to look at the density  $\rho$ , which is shown in Fig. 4. We see that as  $c$  is decreased, the dust is pulled back within the quasihorizon: The fraction of the mass integral of Eq. (2.24) coming from  $r > r_*$  is of order  $(c/q)^{2/3}$ , and vanishes in the critical limit. Curiously, we see that  $\sqrt{A}\rho$  is approximately constant in the interior region.

Finally, in Fig. 5 we show the electric potential  $\phi$  as a function of  $r$ . It is interesting to note how as  $c$  vanishes the profile of  $\phi$  approaches one that is constant in the interior and then falls as  $1/r$  outside the horizon. This clearly illustrates the absence of hair in these solutions.

#### IV. SOLUTIONS WITH HAIR

In the previous section we have used extremal dust to construct a family of spacetimes that come arbitrarily close to having an extremal horizon. As  $c$  tends toward zero, the metric in the region outside the quasihorizon approaches that of an extremal Reissner-Nordström solution. Also, the mass

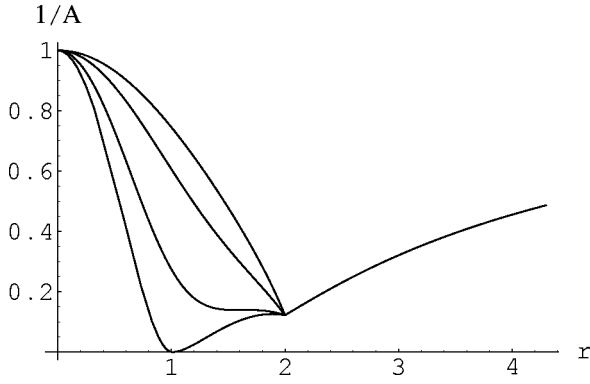


FIG. 6. A plot of  $1/A$  as a function of  $r$  for the case with hair. We have taken  $q=1$ ,  $m=1.3$ ,  $r_b=2$ , and, reading from the top down,  $c=0.5, 0.3, 0.1, 0.001$ . Again the formation of the quasihorizon is quite evident in the  $c=0.001$  curve.

and charge density  $\rho$  tends to zero in this region, so the limiting solution has no hair. In the critical limit  $A$  remains finite and nonsingular inside the horizon, but  $B$  and  $\sqrt{AB}$  both tend toward zero everywhere in the interior region. The sharp jump in  $\sqrt{AB}$  (which becomes a step function in the limiting case) means that an object falling through the quasihorizon is subject to arbitrarily large tidal forces, and that these quasi-black hole solutions can be viewed as “naked black holes” as defined by Horowitz and Ross [16].

All of these properties are similar to those found for the quasi-black hole solutions obtained from magnetic monopoles in theories with weak Higgs self-coupling. However, a second type of quasi-black hole is found in these theories if the Higgs boson self-coupling is larger than a critical value [8,17]. These latter solutions tend toward black holes that are much less singular at the horizon. The metric factor coefficient  $B$  vanishes at the horizon, but then increases again with decreasing  $r$ , and is nonzero throughout the interior region. Similarly,  $\sqrt{AB}$  is everywhere nonzero. Although it decreases rapidly near the horizon, its derivative remains finite and there is no naked-black-hole behavior. Finally, the massive gauge and Higgs fields have tails that extend beyond the horizon, so that the limiting cases of these solutions are black holes with hair.

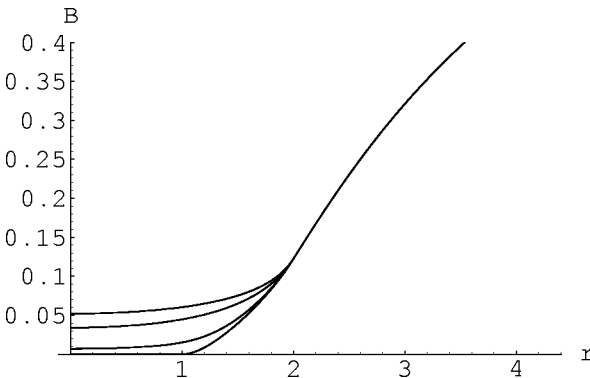


FIG. 7. A plot of  $B(r)$  for the case with hair. We have taken  $q=1$ ,  $m=1.3$ ,  $r_b=2$ , and, reading from the top down,  $c=0.5, 0.3, 0.1, 0.001$ .

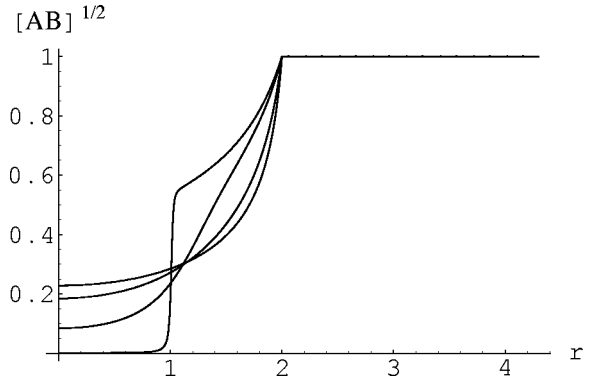


FIG. 8. A plot of  $\sqrt{AB}$  as a function of  $r$  for the case with hair. We have taken  $q=1$ ,  $m=1.3$ ,  $r_b=2$ , and, reading from the top down along the vertical axis,  $c=0.5, 0.3, 0.1, 0.001$ .

It is natural to ask whether extremal dust can also give rise to quasi-black holes with less singular behavior, and whether they can have hair. We begin by noting that the vanishing of  $B$  at any horizon implies that  $U$  must diverge at the horizon. Since  $r=RU$  must remain finite, the horizon must lie at  $R=0$ , just as in the Reissner-Nordström case. This means that in the corresponding quasi-black holes the range  $0 \leq r \leq r_*$  must be mapped into an interval  $0 \leq R \leq R_*$  that is shrinking to a point. Hence,

$$\frac{dR}{dr} = \left[ \frac{d(UR)}{dR} \right]^{-1} = \sqrt{AB} \quad (4.1)$$

must tend to zero everywhere within the quasihorizon, and in the limiting case both  $B$  and  $\sqrt{AB}$  must vanish identically in the interior.

To see whether there can be hair, we must examine the behavior of  $\rho$  near the horizon. We combine Eqs. (2.16) and (2.18) (with  $\rho_e = \rho$ ) to obtain

$$4\pi\rho(1-r\varphi') = \frac{1}{r^2} \left( \frac{r^2\varphi'}{A} \right)'. \quad (4.2)$$

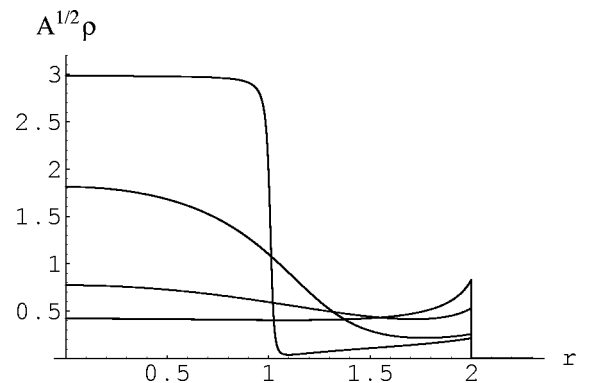


FIG. 9. A plot of  $\sqrt{A}\rho$  as a function of  $r$  for the case with hair. We have taken  $q=1$ ,  $m=1.3$ ,  $r_b=2$ , and, reading from the bottom up along the vertical axis,  $c=0.5, 0.3, 0.1, 0.001$ .

The right-hand side vanishes at an extremal horizon. Since  $\varphi' = -d(\sqrt{B})/dr$  also vanishes at the horizon, the second factor on the left-hand side is nonzero, and so  $\rho = 0$  at the horizon.

However, this does not quite rule out the possibility of hair, since it does not preclude  $\rho$  from being nonzero at points other than the horizon. As an example of this, let us consider modifying our previous ansatz for  $U(R)$  to

$$U_{\text{in}} = 1 + \frac{q}{\sqrt{R^2 + c^2}} + a - b\sqrt{R^2 + c^2}. \quad (4.3)$$

Here  $a$  and  $b \geq 0$  are constants, with  $b$  giving a rough measure of the amount of hair. If we applied this ansatz for all positive values of  $R$ , we would find that the Schwarzschild coordinate  $r = RU(R)$  was not a monotonically increasing function at large  $R$ . To avoid this, we apply Eq. (4.3) only to the region  $R < R_b$ , and at  $R = R_b$  match the solution to an extremal Reissner-Nordström solution with

$$U_{\text{out}} = 1 + \frac{m}{R}. \quad (4.4)$$

In order to be able to match these two solutions without needing a thin shell of matter at the junction, we must require that  $U$  and  $dU/dR$  both be continuous at  $R_b$ . Applying these conditions to Eqs. (4.3) and (4.4) fixes the values of  $a$  and  $b$  to be

$$a = -\frac{2q}{\sqrt{R_b^2 + c^2}} + \frac{m}{R_b^3}(2R_b^2 + c^2), \quad (4.5)$$

$$b = -\frac{q}{R_b^2 + c^2} + \frac{m}{R_b^3}\sqrt{R_b^2 + c^2}. \quad (4.6)$$

With these conditions satisfied, it is straightforward not only to show that  $r$  is a monotonically increasing function of  $R$ , but also to verify that  $\rho$  is everywhere positive.

As before, we should pass to Schwarzschild coordinates  $(t, r, \theta, \phi)$ , and obtain the metric functions  $A$  and  $B$ . Equations (2.15), (4.3), and (4.4) lead to

$$\frac{1}{\sqrt{A}} = \begin{cases} 1 - \frac{R^2[q + b(R^2 + c^2)]}{(R^2 + c^2)[q + (1-a)\sqrt{R^2 + c^2} - b(R^2 + c^2)]}, & R < R_b, \\ \frac{R}{R+m}, & R > R_b, \end{cases} \quad (4.7)$$

where  $R$  should be viewed as an implicit function of  $r = RU(R)$ ; for  $R \geq R_b$ , we have the simple relation  $R = r - m$ .

As with the solutions without hair, we illustrate the approach to the critical limit by plotting a series of solutions with decreasing values of  $c$ . In doing this, we keep the pa-

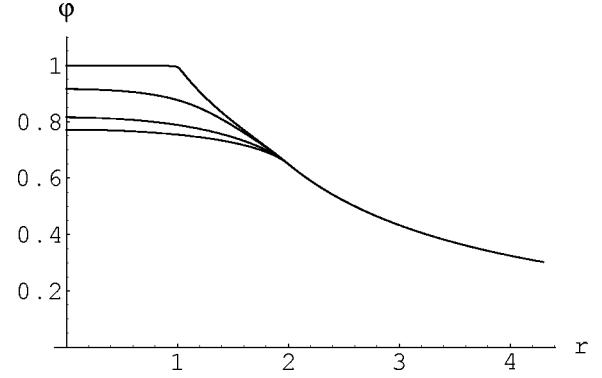


FIG. 10. A plot of  $\varphi(r)$  for the case with hair. We have taken  $q=1$ ,  $m=1.3$ ,  $r_b=2$ , and, reading from the top down,  $c=0.5, 0.3, 0.1, 0.001$ . Even in the limiting case, the decrease of  $\varphi$  from  $r=1$  to  $r=2$  is slower than  $1/r$ , reflecting the presence of charged hair.

rameters  $q$ ,  $m$ , and  $r_b = R_b + m$  fixed. This implies that  $a$  and  $b$  vary so as to satisfy Eqs. (4.5) and (4.6).

In Fig. 6 we plot  $1/A$  as a function of  $r$ . Its behavior is again just as expected, starting from unity at the origin, decreasing to a minimum value, and then increasing at intermediate distances, where it joins<sup>4</sup> on to the extreme Reissner-Nordström solution that tends to an asymptotic value of unity. It remains nonsingular in the critical limit, differing from the extremal Reissner-Nordström solution in not having a singularity at  $r=0$ , and also differing from the  $b=0$  case in that it has hair. The function  $B = 1/U^2$  is shown in Fig. 7. For a black hole,  $B$  should vanish at the horizon. As in the case without hair,  $B$  does not have a minimum at the quasihorizon, but rather decreases monotonically as  $r \rightarrow 0$ . In the limiting case,  $B$  is identically zero for all  $r < r_*$ . At infinity,  $B$  tends to unity. Similarly,  $\sqrt{AB}$ , shown in Fig. 8, also vanishes identically in the interior region in the critical limit. Hence, although we have a nonsingular spacetime for all nonzero  $c$ , the limiting case  $c=0$  is again not itself a smooth manifold.

It is also interesting to look at the density

$$\rho = \frac{1}{4\pi} \frac{3c^2q + b(2R^4 + 5c^2R^4 + 3c^4)}{(R^2 + c^2)[q + (1-a)\sqrt{R^2 + c^2} - b(R^2 + c^2)]^3} \times \Theta(R_b - R). \quad (4.8)$$

The function  $\sqrt{A}\rho$  is shown in Fig. 9. As before, we see that the dust is pulled back within the quasihorizon as  $c$  decreases. However, in contrast to the previous case, the density does not vanish outside the horizon even in the critical limit. It is zero at the quasihorizon, but non-zero inside and outside this surface. We also see that  $\sqrt{A}\rho$  is again approximately constant in the interior region.

The presence of hair can also be seen in the plot of the electric potential  $\varphi(r)$  in Fig. 10. Even in the limiting case

<sup>4</sup>Note that while  $A$  is continuous at this junction, its derivative need not be.

$c \rightarrow 0$ , the falloff of  $\varphi$  in the region  $1 < r < 2$  is slower than  $1/r$ , reflecting the presence of charged hair in this region. Only for  $r > 2$  does the field have the pure Coulomb behavior.

## V. CONCLUDING REMARKS

In this paper we have studied a class of solutions, which we have termed quasi-black holes, that can be viewed as interpolating between nonsingular spacetimes and true black holes. Although these solutions are everywhere nonsingular, they can come arbitrarily close to having horizons, in the sense that the time required for an external observer to distinguish them from a true black hole can be made arbitrarily large. We have focused on solutions constructed from extremal dust—pressureless matter with equal charge and energy densities—and have compared these with the previously studied quasi-black hole solutions based on magnetic monopole soliton solutions. As in the latter case, it is possible to

construct solutions both with and without hair. However, in contrast with the monopole case, the hair is more constrained: In the critical limit, the matter density precisely at the horizon must vanish. Furthermore, we find that the hair does not soften the singularities of the solution to the same extent that it does in the monopole case. Whether the hair is present or not, the solutions display naked-black-hole behavior, with tidal forces that diverge as the critical limit is approached, and the interior solution in the limiting case does not give a smooth manifold.

## ACKNOWLEDGMENTS

This work was supported in part by the U.S. Department of Energy. E.J.W. would like to thank the Aspen Center for Physics, where part of this work was done. J.P.S.L. would like to thank the Portuguese Science Foundation FCT and FSE for support, through POCTI along the III Quadro Comunitário de Apoio, reference number 327/2002.

- 
- [1] A. Lue and E.J. Weinberg, *Phys. Rev. D* **61**, 124003 (2000).
  - [2] A. Lue and E.J. Weinberg, *Gen. Relativ. Gravit.* **32**, 2113 (2000).
  - [3] K. Lee, V.P. Nair, and E.J. Weinberg, *Phys. Rev. D* **45**, 2751 (1992).
  - [4] M.E. Ortiz, *Phys. Rev. D* **45**, 2586 (1992).
  - [5] P. Breitenlohner, P. Forgacs, and D. Maison, *Nucl. Phys.* **B383**, 357 (1992).
  - [6] P. Breitenlohner, P. Forgacs, and D. Maison, *Nucl. Phys.* **B442**, 126 (1995).
  - [7] P.C. Aichelburg and P. Bizon, *Phys. Rev. D* **48**, 607 (1993).
  - [8] A. Lue and E.J. Weinberg, *Phys. Rev. D* **60**, 084025 (1999).
  - [9] S.D. Majumdar, *Phys. Rev.* **72**, 390 (1947).
  - [10] A. Papapetrou, *Proc. R. Ir. Acad., Sect. A* **51**, 191 (1947).
  - [11] W.B. Bonnor and S.B.P. Wickramasuriya, *Mon. Not. R. Astron. Soc.* **170**, 643 (1975).
  - [12] W.B. Bonnor, *Class. Quantum Grav.* **16**, 4125 (1999).
  - [13] J.B. Hartle and S.W. Hawking, *Commun. Math. Phys.* **26**, 87 (1972).
  - [14] A. Das, *Proc. R. Soc. London* **A267**, 1 (1962).
  - [15] B.V. Ivanov, *Phys. Rev. D* **65**, 104001 (2002).
  - [16] G.T. Horowitz and S.F. Ross, *Phys. Rev. D* **56**, 2180 (1997).
  - [17] Y. Brihaye, B. Hartmann, and J. Kunz, *Phys. Rev. D* **62**, 044008 (2000).